PROCEEDINGS OF SCIENCE

Understanding the evolution of Pulsar Wind Nebulae

Barbara Olmi[a,*]

[a] *INAF, Osservatorio Astrofisico di Arcetri, Largo Enrico Fermi 5, Firenze, Italy*

E-mail: barbara.olmi@inaf.it

Pulsar Wind nebulae are visible as bright and extended sources at a wide range of energies, with varying properties and morphology along their different evolutionary stages. For their identification and understanding, it is extremely important to correctly describe the different stages of their evolution, where their dynamics is shaped by the interaction with different actors. Here we will make a brief excursus through the various evolutionary phases, discussing the characteristic properties of a source in a specific phase, and what models have been used for its description.

We will conclude by discussing in particular the last evolutionary stage, that of the bow shock nebula, which is known to be connected with massive particle transfer from the source to the surrounding environment, forming either TeV halos or intriguing misaligned X-ray filaments.

High Energy Phenomena in Relativistic Outflows
23-26 October 2023
Paris, France

*Speaker

1. Introduction

In the supernova explosion of a massive star (with mass $\gtrsim 8M_\odot$), the nucleus of the progenitor generates a compact object, in many cases a rotating neutron star (the pulsar, PSR). Through its decelerated rotation the pulsar produces an outflow, mainly composed by electrons and positrons extracted at the stellar surface or generated in electromagnetic cascades in the magnetosphere, that fills the surrounding medium. This outflow, named pulsar wind, is highly relativistic (with bulk Lorentz factor $\gg 1$), magnetized and cold. The interaction of the pulsar wind with the cold, slowly (300 – 5000 km/s [1]) expanding material of the supernova explosion (the unshocked ejecta) produces an inverse strong magneto-hydrodynamic (MHD) shock, named termination shock (TS). At the TS crossing, randomization heats up the wind plasma, strong magnetic dissipation occurs and particles are accelerated.

Due to the rather large average kick velocity (the velocity inferred at birth) of the pulsar population ($\sim$ 300 km/s [2]), many pulsars are expected to leave their parent supernova remnant bubble at a certain moment of their evolution. For this reason one expects that most of the evolved nebulae directly interact with the interstellar medium (ISM) rather than the ejecta. Nevertheless the picture described above remains almost valid: now the confining material is the ISM, but the PWN still arise from the plasma shocked at the TS, induced by the interaction of the pulsar wind with the ambient material. What changes dramatically is instead the shape of the nebula. While young systems generally appear as fill-centered bubbles, evolved PWNe most likely appear as cometary-like nebulae, with the pulsar located at the bright head of an elongated tail, extending in the direction opposite to the pulsar motion. This is due to the supersonic motion of the pulsar in the ambient medium, that produces a bow shock enclosing and re-shaping the nebula.

Due to its physical properties, the pulsar wind is not directly observable, since it does not produces sizeable luminosity, and it might be identified with the sub-luminous region surrounding the pulsar. The observable PWN then arises from the shocked pulsar wind, where the physical conditions of the plasma are now such as to produce emission via non-thermal radiation mechanisms. The main emission process is synchrotron radiation produced by relativistic particles interacting with the nebular magnetic field, generally with intensity of tens to hundreds of μG. The secondary emission is the radiation produced as consequence of the inverse Compton scattering (ICS) of the available photons with the same relativistic leptons of the nebular plasma. Generally the major contribution comes from photons of the cosmic microwave background (CMB), but also thermal photons and synchrotron photons can be relevant. PWNe are characterized by an extremely broad band spectrum, with emission from radio energies up to hundreds of TeVs (or even PeVs in some cases, as recently discovered by the LHAASO collaboration [3, 4]), where from radio to X-rays the emission is produced through synchrotron radiation, while higher energies come from ICS.

The picture starts to differ from this general one for evolved systems: the lower energy injection from the pulsar, the synchrotron cooling of the leptons and the variation of the value of the nebular magnetic field can lead to the complete vanishing of X-ray emission, while the ICS component might become the dominant one.

From the observational point of view most of the sources identified so far as PWNe were first detected in the X-ray band. This is due to the combination of the impressive sensitivity of the Chandra X-ray telescope for imaging, and to the fact that in the Galaxy the number of other extended and bright sources in this band is very limited, making then easier the identification of a PWN. Unfortunately the X-ray component is the first to fade away as the age of the source passes by. For many aged systems we have no, or very limited (both spatially and in brightness) X-ray emission. On the other hand imaging at radio energies suffers the lack of sensitivity of most radio interferometers, especially in case of evolved systems that require large angular scales. Moreover the extended radio emission might be contaminated by diffuse emission from the surroundings.

PWNe live longer as gamma-ray emitters, where we expect to detect most of the old systems. In fact at this energies the emission is produced by the same population of long-living leptons responsible for the synchrotron radio emission. Regretfully the resolution of the instruments in this band is much worst than that of those looking at lower energies, making almost impossible to perform morphological studies. This problem will be partially mitigated with the advent of the next generation of Imaging Atmospheric Telescopes (IACTs), as the Cherenkov Telescope Array (CTA [5]) and the ASTRI Mini-Array [6], that will have much better spatial and energy resolutions than present instruments, allowing for numerous new discoveries. And in fact the expected number of new detections in the Galaxy is large ($\sim$ 250 [7, 8]), and it poses the problem of the firm identification of a large number of new PWNe, mostly based only on gamma-ray data. Without the possibility of an easy match of most of these sources with their lower energy counterparts (due to their age), this will not be an easy task, and represent a real challenge of the next future very high energy astronomy.

For what has been discussed so far, it should appear clear that PWNe have different properties – and morphology – in the various phases of their life. It is then extremely important to approach each one phase correctly, especially in the view of the spectro-morphological description of a source through the electromagnetic spectrum and its evolution.

2. The phases of PWNe evolution

We can roughly identify three different phases (for an extended discussion see [9]) in the evolution of a PWN, represented in the sketch shown in Fig. 1:
(A) Free-expansion phase;
(B) Reverberation phase;
(C) Late phase, in Fig. 1 shown with the bow-shock phase.
The duration of each of these phases, that we are going to describe in the following, strongly depends on the dynamics of the SNR and the time variation of the pulsar spin-down luminosity, given by:

$$L(t) = L_0 \left(1 + \frac{t}{\tau_0}\right)^{-(n+1)/(n-1)} , \tag{1}$$

where L_0 is the initial luminosity, τ_0 the initial spin-down time and n the braking index. This is generally set to the value representative of the pure dipole, $n = 3$, but large variations have been seen through the pulsar population [10]. From Eq. 1 one can immediately see that the pulsar input can be considered as almost constant only for the limited time $t \ll \tau_0$.

(A) The free-expansion phase:
In the first phase the PWN expands with mild acceleration in the cold and freely expanding ejecta of

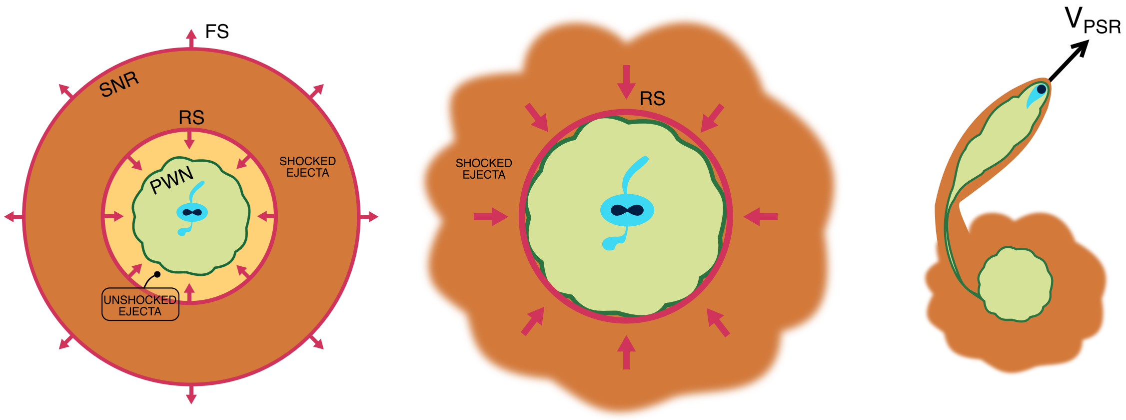

Figure 1: Sketch showing the three main evolutionary stages of PWNe. In the free expansion phase (A) the PWN expands with mild acceleration in the freely expanding supernova remnant (SNR), separated by the ISM through the forward shock (FS). The reverse shock (RS) of the supernova explosion is still travelling through the ejecta, towards the center of explosion. When the RS hits the PWN contact discontinuity the second phase starts: the so called reverberation phase (B). Now the SNR and the PWN are in direct contact. How the system escape this phase strongly depends on the energetics of the combined system SNR+PWN. In the very last evolutionary phase many PWNe will be escaped from their SNR to form bow shock nebulae (C). A relic bubble of radio particles may be left behind the runaway pulsar. The figure has been adapted from [9].

the SNR. Being the PWN expansion speed ($\sim$ few $\times\, 10^3$ km/s) much larger than the typical velocity of the PSR ($\sim 100 - 500$ km/s [2]), at this stage the PSR can be safely considered as at rest in the remnant. At this stage the PWN and the surrounding SNR are not in direct interaction, despite for the fact that the ejecta confine the nebula [11].

The free-expansion phase has been described with a plethora of different approaches, from the simplified one-zone models [12–14], to multi-dimensional MHD simulations [15–20]. For a detailed description of all methods we refer the reader to Olmi & Bucciantini 2023 [9]. The original formulation of one-zone models is based on the same simplified assumption, known as *thin-shell approximation* [11, 13, 21–23]. As the PWN expands in the ejecta of the parent star, it accumulates material at its contact discontinuity, in the form of a swept-up shell. In the aforementioned approximation, this shell is assumed to be infinitely thin, and then used to trace the PWN radius. The evolution of the PWN is then given by the evolution of this thin shell, and it can be easily computed solving the momentum conservation for the shell. Despite their over-simplification of the problem, one-zone models are still the wider used nowadays. The reason is twofold: from the one side they permit to reproduce the approximate evolution of a system in a very short computational time if compared with MHD models; on the other, they make possible to consistently evolve the spectral properties of the PWN particles together with its (approximated) dynamics. This is a missing tool in MHD models, where generally the spectral properties are computed in the post-processing using some kind of recipe to account for the history of the radiative losses. Moreover one-zone models have been shown to be able to account correctly for the global properties of young systems. Of course, if one is interested in the morphology and small scale structures of the PWN, the use of 3-dimensional (3D) MHD models is mandatory.

From the observational point of view, systems in this phase are visible at multi-wavelengths, and their identification is generally made through X-ray imaging.

(B) The reverberation phase:
This phase begins when the reverse shock of the supernova explosion finally hits the border of the PWN (its contact discontinuity). The duration of the previous free-expansion phase depends on how much energetic the pulsar is. An upper limit is set by the reverse shock implosion time $t_{\rm implo}$, that depends on the properties of the ejecta, i.e. their density profile, [24]. The most considered case is that of a flat core plus a steep envelope, for which one gets: $t_{\rm implo} \simeq 2.4 t_{\rm ch}$. Here $t_{\rm ch}$ is the SNR characteristic time [25], defined in terms of the mass of the ejecta $M_{\rm ej}$, the supernova energy $E_{\rm sn}$ and the density of the ISM $\rho_{\rm ISM}$ as: $t_{\rm ch} = M_{\rm ej}^{5/6} E_{\rm sn}^{-1/2} \rho_{\rm ISM}^{-1/3} \simeq 3241\,{\rm yr}\,(M_{\rm ej}/10 M_{\odot})^{5/6}(E_{\rm sn}/10^{51}{\rm erg})^{-1/2}(\rho_{\rm ISM}/1{\rm particle\,cm^{-3}})^{-1/2}$.

When reverberation begins, the PWN and the SNR start to be in direct contact, and the following evolution depends on the properties of both. The pressure exerted by the shocked ejecta on the PWN induces a deceleration of the massive shell of material accumulated at the PWN boundary [26] which, in many cases, turns into a compression of the PWN. The intensity of this compression depends on the energetic of the composite PWN+SNR system. During compression the magnetic field and the internal energy of the PWN both increase. Depending on the importance of magnetic dissipation and radiative losses in this phase, the internal pressure can rise enough to equal the outer one, reverting the compression into a new expansion.

This phase has been investigated mainly through one-zone radiative models [9, 13, 14, 24, 27], essentially because it requires to reproduce a long evolution of the PWN and its SNR, very hard to get with multi-dimensional models. Moreover it also requires the radiative properties of the nebular particles to be evolved consistently with the dynamics and, as we mentioned before, this is still not possible with MHD simulations. One-zone models predict a number of subsequent compressions and expansions during this phase (hence the name *reverberation*); actually this extended oscillatory behaviour is an artifact of the one dimensional approximation [27], while in the multi-dimensional case the onset of Rayleigh-Taylor like instabilities at the PWN border produces an effective mixing of the nebular material with the outer one [28, 29], that acts as a sort of viscous term halting the oscillations after the first compression.

While the thin-shell approximation at the base of one-zone models maps very well the evolution during the free-expansion phase, this is no more true when entering reverberation, because the shell cannot – in general – be approximated as thin anymore [30]. This, especially for moderate compressive systems, might produce substantial artifacts in the spectral evolution of the source, with a clear bias in our interpretation of the faith of a system on a long term timeline. Bandiera et al. [31] recently presented an hybrid Lagrangian/one-zone model to overcome these limitations. They used a Lagrangian technique to map the shell evolution, together with the usual time-dependent radiative model for the spectral properties of the PWN. While results for the the free-expansion phase remain unchanged, substantial differences arises at later times if comparing with the standard one-zone evolution, especially for the low compressive systems, while it is less critical for highly-compressible cases.

The outcome of the reverberation phase can be roughly divided into two extreme cases: (i) the PWN is energetic enough that the effect of the compression is almost not appreciable, and the nebula continues its expansion; (ii) the PWN is faint and it is overwhelmed by the external pressure, contracting down to very small radii. This violent compression might produce important modifications of the PWN spectral properties at multi-wavelengths. In case of extreme compressions (where the PWN radius is reduced by a factor $\gtrsim 1000$ with respect to its value at the begging of reverberation), the PWN can enter a fast cooling regime, where a large fraction of the particles are lost through radiation and their energy distribution is strongly modified [32, 33]. This has been shown to be a rather uncommon case, possibly affecting only a limited number of systems in the PWN population [30].

Observationally is not an easy task to firmly identify systems facing this interactive state. Nowadays we have only identified a handful of objects in reverberation: the Boomerang nebula [34], the Snail [35, 36] and Vela X [28]. The non-spherical interaction of the PWN with the reverse shock, the presence of the Rayleigh-Taylor instability at the PWN boundary and the pulsar proper motion are likely to form very asymmetric systems. The original nebula might be fragmented with radio (and gamma-ray) emitting bubbles detached from the PWN and surrounding the real nebula. These relic bubbles do not evolve anymore, they are only subject to adiabatic expansion.

(C) Late phases and evolved PWNe:
Thus after reverberation PWNe are likely to show important asymmetries. For this reason this phase cannot be modeled with simplified – by assumption spherical – one-zone models, and it requires a full 3D modeling. This is of course very difficult with present models/facilities, since to reach this phase one has to simulate all the previous evolutionary stages, while at present models are only able to reproduce a very limited part of the evolution. Moreover the number of possible targets to tune models is very limited, since it is not easy to detect and recognize PWNe in this phase; the number of identified sources with a detailed characterization is very limited [36–40].

As we mentioned in the introduction, due to the large average kick velocity of the pulsar population [2], many systems are fated to escape their parent SNR before their spin-down luminosity gets so low that acceleration of particles and radiative processes become negligible. Once escaped, those pulsars interact directly with the ambient medium, the ISM in general, where their motion suddenly becomes supersonic, given that the speed of sound in the medium is much lower than the pulsar speed. This gives rise to the formation of a bow shock PWN (BSPWN hereafter), a nebula shaped by the bow shock that forms at the boundary with the outer medium, and that re-shapes the PWN in a cometary like fashion: the pulsar is now located at the bright head of an elongated tail, extending in the direction opposite to the pulsar motion. This peculiar shape is determined by the balance of the ram pressure of the pulsar wind with that of the ambient medium (seen as an incoming flow in the pulsar reference frame). This balance also determines the thickness of the bow shock immediately in front to the pulsar motion, which is known as the *stand-off distance*: $d_0 = [L(t)/(4\pi c\, \rho_{\rm ISM}\, v_{\rm PSR})]^{1/2}$. Here c is the speed of light and $v_{\rm PSR}$ the velocity of the pulsar.

To date we know about 25 systems in this phase, mainly discovered at X-rays (hence associated to still quite luminous pulsars), in some cases then also detected in the radio band, with even more extended wind tails. If the ambient medium is partially ionized, the bow shock can be detected in

H_α emission. No TeV emission has been detected in direct association with such sources for the moment.

Anisotropies in the ambient medium density easily reflects in modifications of the large scale bow shock morphology [41]. On the other hand, even large modifications in the properties of the pulsar wind at injection, have mild effect on the global structure of the bow shock: they mostly affect the morphology in the head region, typically poorly resolved even in the deepest Chandra's observations [42, 43]. Most important for the dynamical properties of the BSPWN and its emitting and polarization properties [43] is the level of turbulence that develops in the shocked pulsar wind. This depends on the distribution of the energy flux and the initial magnetization level of the wind [44]: the lower is magnetization, the higher is the level of turbulence developed in the system, at odds with the wind anisotropy. At fixed magnetization, the turbulence is higher the higher is anisotropy.

3. Formation of structures around bow shock nebulae

In recent years BSPWNe have regained attention due to the increasing number of sources showing puzzling misaligned and extremely thin X-ray features produced close to the head and extending in the ambient medium for long distances ($\sim 1-15$ pc), somehow resembling a jet or a filament. This kind of feature was first detected in the Guitar Nebula in the first decade of the millennium [45], and soon after interpreted as produced by particles of very high energy (close to the maximum theoretical limit of the pulsar potential drop) escaping the bow shock nebula and emitting synchrotron radiation in the ambient magnetic field [46]. In all cases the magnetic field in correspondence of the feature needs to be much larger than the standard value of the unperturbed ISM ($\sim 5\,\mu$G), with values of 20-50 μG required to explain the observed emission around the keV.

A decade after, the mechanism through which high energy particles escape the BSPWN and stream away along the ambient magnetic field lines was finally proved. Bucciantini [47] showed that particles can remain confined into current sheets and current layers from their injection region. Then, depending on the geometry of the system, the current sheet may transport those particles at the contact discontinuity. This mechanism is also naturally able to produce important anisotropies of the charge distribution in the escaping flow. As we will see later, this is a fundamental aspect for the interpretation of the nature of the X-ray filaments.

Soon later, 3D relativistic numerical simulations of BSPWNe showed that reconnecting regions between the nebular magnetic field and the ordered ambient one are common to develop and persist [48]. From the vicinity of those reconnection regions at the magnetopause, particles can then jump in the outer magnetic field, depending on the specific geometry of the system [44]. The escape process is energy dependent: the lower is the particle energy, the smaller is its Larmor radius, and then the particle can only escape if it intercepts directly a reconnection point. On the contrary, higher energy particles have larger Larmor radii, and for them it is sufficient to be close enough to a reconnection point to be able to jump outside. Roughly speaking, one can expect that the escape process is much more efficient for particles having a Larmor radius $\sim d_0$, meaning particles with an energy which is a consistent fraction of the maximum available one (that associated with the pulsar potential drop) [49].

Once escaped, particles interact with the ambient magnetic field, illuminating its structure through synchrotron radiation. As mentioned above, the observed emission is compatible with synchrotron radiation emitted by very high energy leptons interacting with a magnetic field substantially larger (of a factor of ~ 10) than the typical ISM one. This is a possible indication of an instability generated by the escaping particles that amplifies the ambient magnetic field [49].

In [50] the authors show that the length, transverse dimension and X-ray luminosity of a selection of X-ray filaments can be accounted for if a non-resonant hybrid instability [51] is excited. This requires specific conditions to be fulfilled, namely: (i) high energy electrons and positrons are spatially charge separated while leaving the bow shock [44]; (ii) they escape in a number sufficient to excite the non resonant hybrid instability. The current density can be increased if the escaping particles are focused in a narrow angle at their escaping point: this in fact confines the particles in a region with a small cross section. Since the instability is non resonant, the particles that power the current can stream away from the bow shock without being scattered for a distance $L_f \sim c\tau_{CR}$, where τ_{CR} is the time the instability needs to reach saturation. During this time the magnetic field keeps growing on scales much smaller than the Larmor radius of the current dominating particles. When saturation is reached, power is driven on larger scales because of the nonlinear evolution of the instability [51], eventually up to scales comparable with the Larmor radius of the current driving particles. Now particles start to scatter and rapidly reach isotropization. The observed X-ray emission then is produced by these isotropized particles interacting with the amplified magnetic field along L_f.

This mechanism can lead in general to confinement of particles around sources, even in extended regions, with important implications on the contribution of pulsars to cosmic ray leptons [52]. Moreover evolved pulsars are associated also with the formation of extended TeV halos [53], that have been interpreted as produced by particles escaped from the source and diffusing in the surrounding, with some suppression of the standard galactic diffusion coefficient. One may speculate that a similar process is acting in those regions, powering a turbulence responsible for the suppression of the diffusion.

4. Concluding remarks

Pulsar Wind Nebulae are bright and intriguing systems, visible across the electromagnetic spectrum, from radio to gamma-rays, with variations depending on their evolutionary stage. Their multi-faced properties require complex physics to be described and to date a unified model able to account for all the aspects through the complete evolution of a PWN still lack. Here we have discuss which is the most used approach for the different phases, and which results one can safely extract.

PWN are known to be efficient antimatter factories and particle accelerators, possibly the main sources of the positron excess measured in the cosmic ray spectrum at Earth. The Crab Nebula, a young PWN considered the class prototype, is to date the unique firmly identified leptonic PeVatron in the Galaxy. Nevertheless LHAASO recently detected a number of PeV emitting sources [3], whose nature, in most cases, seems to be associated with a pulsar [54].

Great attention have been regained recently by evolved PWNe confined by the interstellar medium (bow shock nebulae), since peculiar extended X-ray filaments have been seen around a number of these sources, thanks to dedicated deep observations with Chandra. The most famous and well resolved cases are those of the Guitar nebula [45] and the Lighthouse nebula [55]. These X-ray filaments can be interpreted as produced by the non-resonant hybrid streaming instability self-generated by the escaping particles, that produce an important amplification of the ambient magnetic field. Once the instability reaches saturation, the particles start to scatter and rapidly isotropize, being then able to produce the observed emission. The same mechanism might be more in general at the base of the confinement of particles around sources in the Galaxy and related to the formation of extended TeV halos recently discovered around a few evolved pulsars.

Acknowledgments

The author wish to acknowledge all the colleagues that contribute to the work presented in this proceeding, in particular: Elena Amato, Rino Bandiera, Niccolò Bucciantini and Pasquale Blasi. The author also acknowledges support by the Italian National Institute for Astrophysics grant PRIN-INAF 2019.

References

[1] R.A. Chevalier, *The hydrodynamics of type II supernovae.*, *ApJ* **207** (1976) 872.

[2] C.-A. Faucher-Giguère and V.M. Kaspi, *Birth and Evolution of Isolated Radio Pulsars*, *ApJ* **643** (2006) 332 [astro-ph/0512585].

[3] Z. Cao, F.A. Aharonian, Q. An, L.X. Axikegu, Bai, Y.X. Bai, Y.W. Bao et al., *Ultrahigh-energy photons up to 1.4 petaelectronvolts from 12 γ-ray Galactic sources*, *Nature* **594** (2021) 33.

[4] Z. Cao, F. Aharonian, Q. An, Axikegu, L.X. Bai, Y.X. Bai et al., *Peta-electron volt gamma-ray emission from the Crab Nebula*, *Science* **373** (2021) 425 [2111.06545].

[5] M. Actis, G. Agnetta and e.a. Aharonian, *Design concepts for the Cherenkov Telescope Array CTA: an advanced facility for ground-based high-energy gamma-ray astronomy*, *Experimental Astronomy* **32** (2011) 193 [1008.3703].

[6] S. Scuderi, A. Giuliani, G. Pareschi, G. Tosti, O. Catalano, E. Amato et al., *The ASTRI Mini-Array of Cherenkov telescopes at the Observatorio del Teide*, *Journal of High Energy Astrophysics* **35** (2022) 52.

[7] M. Fiori, B. Olmi, E. Amato, R. Bandiera, N. Bucciantini, L. Zampieri et al., *Modelling the γ-ray pulsar wind nebulae population in our galaxy*, *MNRAS* **511** (2022) 1439 [2201.02221].

[8] Q. Remy, L. Tibaldo, F. Acero, M. Fiori, J. Knödlseder, B. Olmi et al., *Survey of the Galactic Plane with the Cherenkov Telescope Array*, in *37th International Cosmic Ray Conference*, p. 886, Mar., 2022, DOI [2109.03729].

[9] B. Olmi and N. Bucciantini, *The Dawes Review 11: From young to old: The evolutionary path of Pulsar Wind Nebulae*, *PASA* **40** (2023) e007 [2301.12903].

[10] A. Parthasarathy, S. Johnston, R.M. Shannon, L. Lentati, M. Bailes, S. Dai et al., *Timing of young radio pulsars - II. Braking indices and their interpretation*, *MNRAS* **494** (2020) 2012 [2003.13303].

[11] S.P. Reynolds and R.A. Chevalier, *Evolution of pulsar-driven supernova remnants.*, *ApJ* **278** (1984) 630.

[12] F. Pacini and M. Salvati, *On the Evolution of Supernova Remnants. Evolution of the Magnetic Field, Particles, Content, and Luminosity*, *ApJ* **186** (1973) 249.

[13] J.D. Gelfand, P.O. Slane and W. Zhang, *A Dynamical Model for the Evolution of a Pulsar Wind Nebula Inside a Nonradiative Supernova Remnant*, *ApJ* **703** (2009) 2051 [0904.4053].

[14] D.F. Torres, A. Cillis, J. Martín and E. de Oña Wilhelmi, *Time-dependent modeling of TeV-detected, young pulsar wind nebulae*, *JHEAp* **1** (2014) 31 [1402.5485].

[15] L. Del Zanna, D. Volpi, E. Amato and N. Bucciantini, *Simulated synchrotron emission from pulsar wind nebulae*, *A&A* **453** (2006) 621 [astro-ph/0603080].

[16] N.F. Camus, S.S. Komissarov, N. Bucciantini and P.A. Hughes, *Observations of 'wisps' in magnetohydrodynamic simulations of the Crab Nebula*, *MNRAS* **400** (2009) 1241 [0907.3647].

[17] B. Olmi, L. Del Zanna, E. Amato, R. Bandiera and N. Bucciantini, *On the magnetohydrodynamic modelling of the Crab nebula radio emission*, *MNRAS* **438** (2014) 1518.

[18] B. Olmi, L. Del Zanna, E. Amato and N. Bucciantini, *Constraints on particle acceleration sites in the Crab nebula from relativistic magnetohydrodynamic simulations*, *MNRAS* **449** (2015) 3149.

[19] O. Porth, S.S. Komissarov and R. Keppens, *Three-dimensional magnetohydrodynamic simulations of the Crab nebula*, *MNRAS* **438** (2014) 278 [1310.2531].

[20] B. Olmi, L. Del Zanna, E. Amato, N. Bucciantini and A. Mignone, *Multi-D magnetohydrodynamic modelling of pulsar wind nebulae: recent progress and open questions*, *JPP* **82** (2016) 635820601 [1610.07956].

[21] N. Bucciantini, E. Amato, R. Bandiera, J.M. Blondin and L. Del Zanna, *Magnetic Rayleigh-Taylor instability for Pulsar Wind Nebulae in expanding Supernova Remnants*, *A&A* **423** (2004) 253 [astro-ph/0405276].

[22] J. Martín, D.F. Torres and N. Rea, *Time-dependent modelling of pulsar wind nebulae: study on the impact of the diffusion-loss approximations*, *MNRAS* **427** (2012) 415 [1209.0300].

[23] D.F. Torres, *Rotationally Powered Magnetar Nebula around Swift J1834.9-0846*, *ApJ* **835** (2017) 54 [1612.02835].

[24] R. Bandiera, N. Bucciantini, J. Martín, B. Olmi and D.F. Torres, *Revisiting the evolution of non-radiative supernova remnants: a hydrodynamical-informed parametrization of the shock positions*, *MNRAS* **508** (2021) 3194 [2109.03612].

[25] J.K. Truelove and C.F. McKee, *Evolution of Nonradiative Supernova Remnants*, *ApJS* **120** (1999) 299.

[26] E. van der Swaluw, A. Achterberg, Y.A. Gallant and G. Tóth, *Pulsar wind nebulae in supernova remnants. Spherically symmetric hydrodynamical simulations*, *A&A* **380** (2001) 309.

[27] N. Bucciantini, J. Arons and E. Amato, *Modelling spectral evolution of pulsar wind nebulae inside supernova remnants*, *MNRAS* **410** (2011) 381 [1005.1831].

[28] J.M. Blondin, R.A. Chevalier and D.M. Frierson, *Pulsar Wind Nebulae in Evolved Supernova Remnants*, *ApJ* **563** (2001) 806 [astro-ph/0107076].

[29] C. Kolb, J. Blondin, P. Slane and T. Temim, *Evolution of a Pulsar Wind Nebula within a Composite Supernova Remnant*, *ApJ* **844** (2017) 1 [1707.06352].

[30] R. Bandiera, N. Bucciantini, J. Martín, B. Olmi and D.F. Torres, *Reverberation of pulsar wind nebulae - II. Anatomy of the 'thin-shell' evolution*, *MNRAS* **520** (2023) 2451 [2301.04056].

[31] R. Bandiera, N. Bucciantini, B. Olmi and D.F. Torres, *Reverberation of pulsar wind nebulae - III. Modelling of the plasma interface empowering a long term radiative evolution*, *MNRAS* **525** (2023) 2839 [2307.13491].

[32] D.F. Torres and T. Lin, *Discovery and Characterization of Superefficiency in Pulsar Wind Nebulae*, *ApJLett* **864** (2018) L2 [1808.10613].

[33] D.F. Torres, T. Lin and F. Coti Zelati, *Towards observing reverberating and superefficient pulsar wind nebulae*, *MNRAS* **486** (2019) 1019 [1903.08681].

[34] R. Kothes, W. Reich and B. Uyanıker, *The Boomerang PWN G106.6+2.9 and the Magnetic Field Structure in Pulsar Wind Nebulae*, *ApJ* **638** (2006) 225.

[35] T. Temim, P. Slane, B.M. Gaensler, J.P. Hughes and E. Van Der Swaluw, *Chandra and XMM Observations of the Composite Supernova Remnant G327.1-1.1*, *ApJ* **691** (2009) 895 [0811.0832].

[36] T. Temim, P. Slane, C. Kolb, J. Blondin, J.P. Hughes and N. Bucciantini, *Late-Time Evolution of Composite Supernova Remnants: Deep Chandra Observations and Hydrodynamical Modeling of a Crushed Pulsar Wind Nebula in SNR G327.1-1.1*, *ApJ* **808** (2015) 100 [1506.03069].

[37] D.A. Frail, E.B. Giacani, W.M. Goss and G. Dubner, *The Pulsar Wind Nebula around PSR B1853+01 in the Supernova Remnant W44*, *ApJLett* **464** (1996) L165 [astro-ph/9604121].

[38] R. Petre, K.D. Kuntz and R.L. Shelton, *The X-Ray Structure and Spectrum of the Pulsar Wind Nebula Surrounding PSR B1853+01 in W44*, *ApJ* **579** (2002) 404 [astro-ph/0207092].

[39] D.A. Swartz, G.G. Pavlov, T. Clarke, G. Castelletti, V.E. Zavlin, N. Bucciantini et al., *High Spatial Resolution X-Ray Spectroscopy of the IC 443 Pulsar Wind Nebula and Environs*, *ApJ* **808** (2015) 84 [1506.05507].

[40] Y.K. Ma, C.Y. Ng, N. Bucciantini, P.O. Slane, B.M. Gaensler and T. Temim, *Radio Polarization Observations of the Snail: A Crushed Pulsar Wind Nebula in G327.1-1.1 with a Highly Ordered Magnetic Field*, *ApJ* **820** (2016) 100 [1603.04886].

[41] M. Vigelius, A. Melatos, S. Chatterjee, B.M. Gaensler and P. Ghavamian, *Three-dimensional hydrodynamic simulations of asymmetric pulsar wind bow shocks*, *MNRAS* **374** (2007) 793 [astro-ph/0610454].

[42] B. Olmi and N. Bucciantini, *Full-3D relativistic MHD simulations of bow shock pulsar wind nebulae: dynamics*, *MNRAS* **484** (2019) 5755 [1902.00442].

[43] B. Olmi and N. Bucciantini, *Full-3D relativistic MHD simulations of bow shock pulsar wind nebulae: emission and polarization*, *MNRAS* **488** (2019) 5690 [1907.12356].

[44] B. Olmi and N. Bucciantini, *On the origin of jet-like features in bow shock pulsar wind nebulae*, *Monthly Notices of the Royal Astronomical Society* **490** (2019) 3608 [1910.01926].

[45] C.Y. Hui and W. Becker, *X-ray emission properties of the old pulsar PSR B2224+65*, *A&A* **467** (2007) 1209 [astro-ph/0610505].

[46] R. Bandiera, *On the X-ray feature associated with the Guitar nebula*, *A&A* **490** (2008) L3 [0809.2159].

[47] N. Bucciantini, *A laminar model for the magnetic field structure in bow-shock pulsar wind nebulae*, *MNRAS* **478** (2018) 2074 [1805.01653].

[48] M.V. Barkov, M. Lyutikov, N. Klingler and P. Bordas, *Kinetic 'jets' from fast-moving pulsars*, *MNRAS* **485** (2019) 2041 [1804.07341].

[49] B. Olmi, *Evolved Pulsar Wind Nebulae*, *Universe* **9** (2023) 402 [2309.02263].

[50] B. Olmi, E. Amato, R. Bandiera and P. Blasi, *The nature of the X-ray filaments around bow shock pulsar wind nebulae*, *arXiv e-prints* (2024) arXiv:2403.03616 [2403.03616].

[51] A.R. Bell, *Turbulent amplification of magnetic field and diffusive shock acceleration of cosmic rays*, *MNRAS* **353** (2004) 550.

[52] B. Schroer, C. Evoli and P. Blasi, *TeV halos and the role of pulsar wind nebulae as sources of cosmic-ray positrons*, *Phys. Rev. D* **107** (2023) 123020 [2305.08019].

[53] e.a. Abeysekara, *Extended gamma-ray sources around pulsars constrain the origin of the positron flux at Earth*, *Science* **358** (2017) 911 [1711.06223].

[54] E. de Oña Wilhelmi, R. López-Coto, E. Amato and F. Aharonian, *On the Potential of Bright, Young Pulsars to Power Ultrahigh Gamma-Ray Sources*, *Astrophysical Journal Letters* **930** (2022) L2 [2204.09440].

[55] L. Pavan, P. Bordas, G. Pühlhofer, M.D. Filipović, A. De Horta, A. O'Brien et al., *The long helical jet of the Lighthouse nebula, IGR J11014-6103*, *Astronomy & Astrophysics* **562** (2014) A122 [1309.6792].